Supplementary Information for

Oligo(ethylene glycol)-Incorporated Hole Transporting Polymers for Efficient and Stable Inverted Perovskite Solar Cells

Chulhee Lim[†, a], *Youngwoong Kim* [†, b, c], *Seungjin Lee* [a], *Helen Hejin Park*[b, d], *Nam Joong Jeon*[*, b] *and Bumjoon J. Kim*[*, a]

[a] Department of Chemical and Biomolecular Engineering, Korea Advanced Institute of Science and Technology (KAIST), Daejeon 34141, Republic of Korea

[b] Division of Advanced Materials, Korea Research Institute of Chemical Technology (KRICT), Daejeon 34114, Republic of Korea

[c]Green and Sustainable Materials R&D Department, Korea Institute of Industrial Technology (KITECH), Cheonan, Chungcheongnam 31056, Republic of Korea

[d]Department of Advanced Materials and Chemical Engineering, University of Science and Technology (UST), Daejeon 34113, Republic of Korea

[*]**Electronic mail:** (N. J. Jeon) njjeon@krict.re.kr, (B. J. Kim) bumjoonkim@kaist.ac.kr

Table of Contents

Experimental Section

Supplementary Schemes

Supplementary Fig.s

Supplementary Tables

Experimental Section

Materials

All the chemicals were purchased from Sigma Aldrich, Alfa Aesar, or Tokyo Chemical Industry (TCI) Co. and used without further purification. Compound 1 was synthesized by following the previous literature.[1]

Synthesis

General synthetic procedures for OEG-Tos: Ethylene glycol monomethyl ether (40 mmol) and 40 mL of dichloromethane (DCM) were injected into a 100 mL round-bottom flask. After triethylamine (60 mmol) was added, the solution was stirred for 10 min at room temperature. Finally, *p*-toluenesulfonyl chloride (TosCl) in 20 mL of DCM was added dropwise, and the mixtures were vigorously stirred overnight. The resultant was poured into the deionized (DI) water and extracted with DCM (100 mL) 3 times. After being dried with $MgSO_4$, the organic solvents were completely removed by a rotary evaporator, and the crude product was purified by silica column chromatography.

***2-methoxyethyl 4-methylbenzenesulfonate* (*MEG-Tos*)**: colorless liquid (yield : 95%) ^{1}H NMR (400 MHz, Chloroform-*d*) δ 7.81 – 7.74 (m, 2H), 7.35 – 7.28 (m, 2H), 4.17 – 4.10 (m, 2H), 3.58 – 3.52 (m, 2H), 3.28 (s, 3H), 2.42 (s, 3H).

***2-(2-methoxyethoxy)ethyl 4-methylbenzenesulfonate* (*DEG-Tos*)**: colorless liquid (yield : 96%) ^{1}H NMR (400 MHz, Chloroform-*d*) δ 7.80 – 7.73 (m, 2H), 7.34 – 7.27 (m, 2H), 4.17 – 4.10 (m, 2H), 3.69 – 3.62 (m, 2H), 3.58 – 3.51 (m, 2H), 3.48 – 3.41 (m, 2H), 3.31 (s, 3H), 2.41 (s, 3H).

***2-(2-(2-methoxyethoxy)ethoxy)ethyl 4-methylbenzenesulfonate* (*TEG-Tos*)**: colorless liquid

(yield : 92%) ^{1}H NMR (400 MHz, Chloroform-*d*) δ 7.81 – 7.74 (m, 2H), 7.35 – 7.28 (m, 2H), 4.17 – 4.10 (m, 2H), 3.70 – 3.63 (m, 2H), 3.62 – 3.55 (m, 6H), 3.55 – 3.47 (m, 2H), 3.35 (d, J = 0.5 Hz, 3H), 2.42 (s, 3H).

Compound 2: The compound 1 (1 g, 2.16 mmol) in a 100 mL round-bottom flask was dissolved by 30 mL of DCM. Then, the temperature of the resultant solution was maintained at −78 ℃. An excessive amount of 1M of boron tribromide (BBr_3) solution (6.92 mL, 6.92 mmol) (diluted in DCM) was injected, and the resultant solution was stirred at −78 ℃. After 3 h, the solution was poured into the ice to slowly quench the unreacted BBr_3. When the color of the solution changed to bright yellow, the crude product was extracted with DCM (100 mL) 3 times and dried over $MgSO_4$. After removing the residual solvent by a rotary evaporator, silica column chromatography was conducted to produce a white solid (0.89 g, 86%). ^{1}H NMR (400 MHz, Dimethyl sulfoxide-d_6) δ 9.49 (s, 1H), 7.37 – 7.30 (m, 4H), 6.81 – 6.74 (m, 4H), 6.53 (s, 2H), 1.83 (d, J = 1.3 Hz, 6H).

General synthetic procedures for OEG-TAA monomers: Compound 2 (2.38 mmol) in 100 mL of a round-bottom flask was dissolved in 30 mL of anhydrous dimethylformamide (DMF) in a N_2 atmosphere. Then, potassium hydroxide (KOH, 5.96 mmol) was quickly added to the solution and stirred for 30 min. After injecting OEG-Tos (4.76 mmol), the mixture was stirred overnight at room temperature. The crude product was washed with DI water and extracted with DCM (100 ml) 3 times. After dried over $MgSO_4$, the remaining organic solvent was removed with a rotary evaporator and the crude product was purified by column chromatography to obtain the final product.

N,N-bis(4-bromophenyl)-4-(2-methoxyethoxy)-2,6-dimethylaniline **(*MEG-TAA*)** : White

solid (yield : 85 %). ^{1}H NMR (400 MHz, Chloroform-*d*) δ 7.25 (dd, *J* = 6.9, 1.9 Hz, 4H), 6.83 – 6.76 (m, 4H), 6.65 (s, 2H), 4.12 – 4.04 (m, 2H), 3.77 – 3.70 (m, 2H), 3.44 (d, *J* = 1.5 Hz, 3H), 1.95 (s, 6H).

N,N-bis(4-bromophenyl)-4-(2-(2-methoxyethoxy)ethoxy)-2,6-dimethylaniline (DEG-TAA) : Colorless liquid (yield : 83 %). ^{1}H NMR (400 MHz, Chloroform-*d*) δ 7.25 (d, *J* = 7.7 Hz, 4H), 6.79 (d, *J* = 8.4 Hz, 4H), 6.65 (s, 2H), 4.11 (t, *J* = 4.9 Hz, 2H), 3.86 – 3.82 (m, 2H), 3.73 – 3.69 (m, 2H), 3.59 – 3.54 (m, 2H), 3.38 (d, *J* = 2.0 Hz, 3H), 1.95 (s, 6H).

N,N-bis(4-bromophenyl)-4-(2-(2-(2-methoxyethoxy)ethoxy)ethoxy)-2,6-dimethylaniline (TEG-TAA) : Colorless liquid (yield : 78 %). ^{1}H NMR (400 MHz, Chloroform-*d*) δ 7.26 (d, *J* = 2.0 Hz, 4H), 6.79 (d, *J* = 8.5 Hz, 4H), 6.65 (s, 2H), 4.10 (t, *J* = 4.8 Hz, 2H), 3.84 (t, *J* = 4.9 Hz, 2H), 3.75 – 3.70 (m, 2H), 3.69 – 3.62 (m, 4H), 3.56 – 3.52 (m, 2H), 3.36 (s, 3H), 1.95 (s, 6H).

General procedures of polymerization for the OEG-PTAA polymers **:** The OEG-PTAA polymers were obtained by the same experimental procedure as the previous literature.[1]

Poly(4-(2-methoxyethoxy)-2,6-dimethyl-N,N-diphenylaniline) (MEG-PTAA) : Light yellow solid (yield : 46%) ^{1}H NMR (400 MHz, *ortho*-Dichlorobenzene-d_4) δ 7.49 (d, *J* = 8.5 Hz, 4H), 7.10 (d, *J* = 8.2 Hz, 4H), 6.69 (s, 2H), 4.02 (s, 2H), 3.72 – 3.61 (m, 2H), 3.33 (d, *J* = 1.7 Hz, 3H), 2.19 – 2.00 (m, 6H).

Poly(4-(2-(2-methoxyethoxy)ethoxy)-2,6-dimethyl-N,N-diphenylaniline) (DEG-PTAA) : Light yellow solid (yield : 42%) ^{1}H NMR (400 MHz, *ortho*-Dichlorobenzene-d_4) δ 7.50 (d, *J* = 8.6 Hz, 4H), 7.10 (d, *J* = 8.2 Hz, 4H), 6.67 (s, 2H), 4.01 (s, 2H), 3.79 (t, *J* = 4.8 Hz, 2H), 3.64 (dd, *J* = 5.7, 3.8 Hz, 2H), 3.48 (dd, *J* = 6.0, 3.6 Hz, 2H), 3.26 (s, 3H), 2.09 (s, 6H).

Poly(4-(2-(2-(2-methoxyethoxy)ethoxy)ethoxy)-2,6-dimethyl-N,N-diphenylaniline) (TEG-PTAA) : Light yellow solid (yield : 40%) ^{1}H NMR (400 MHz, *ortho*-Dichlorobenzene-d_4) δ

7.50 (d, J = 8.8 Hz, 4H), 7.10 (d, J = 8.5 Hz, 4H), 6.67 (s, 2H), 3.99 (s, 2H), 3.77 (d, J = 5.0 Hz, 2H), 3.67 – 3.51 (m, 6H), 3.43 (t, J = 4.8 Hz, 2H), 3.21 (d, J = 3.8 Hz, 3H), 2.09 (s, 6H).

Characterization

^{1}H nuclear magnetic resonance (NMR) measurement was conducted with Bruker AVANCE III HD Nanobay (9.4 T) instrument using chloroform-*d* (7.24 ppm), dimethyl sulfoxide-d_6 (2.50 ppm) and *ortho*-dichlorobenzene-d_4 (7.19 and 6.93 ppm) as solvents. The number average molecular weights (M_ns) and polydispersity ($Đ$) of the HTMs were measured by size exclusion chromatography (SEC) against polystyrene standards using HPLC grade tetrahydrofuran (THF) as an eluent (1 mL min^{-1} at room temperature) (Waters 1515 isocratic HPLC pump, 2707 auto sampler, and 2414 refractive index detector). UV-Vis absorption and transmittance spectra were measured with Shimadzu Scientific UV-1800 spectrophotometer. Photoluminescence (PL) spectra were measured with HORIBA SCIENTIFIC Fluorolog-3 with single photon counting photomultiplier tube (PMT) at room temperature. Photoelectron spectroscopy in air (PESA) measurements were conducted with Riken Keiki AC-2 photoelectron spectrometer. Contact angle measurement was conducted with Surface Electro Optics Phoenix 300 Touch model. X-ray photoelectron spectroscopy (XPS) measurement was carried out with Thermo Scientific Instrument Nexsa G2 surface analysis system. Scanning electron microscope (SEM) images were obtained with FE-SEM (Tescan Mira 3 LMU FEG, 10 kV). The X-ray diffraction (XRD) spectra were obtained by a Rigaku Smart Lab X-ray diffractometer. External quantum efficiency (EQE) measurements were performed using Newport system, QuantX-300 (Newport). Time correlated single photon counting (TSCPC) measurements were carried out by Edinburgh Instruments, FL920. The samples were excited at 470 nm and the PL decays were detected at 780 nm.

Current density-voltage (*J-V*) curves were recorded using a solar simulator (Newport, Oriel Class A, 91195A) with Keithley 2420 source meter under illumination at AM 1.5G. The solar simulator is calibrated using a Si-reference cell certificated by National Renewable Energy Laboratory (NREL). All devices were measured with a metal mask with an active area of 0.094 cm^2. The step voltage and delay time were fixed at 10 mV and 10 ms, respectively.

Fourier transform infrared (FTIR) spectra were measured by Thermo Fisher Scientific Instrument Nicolet iS50 model with attenuated total reflection (ATR) mode. For sample preparation, pristine HTMs and PbI_2 with a weight ratio of 1 to 2 were dissolved together in tetrahydrofuran (THF) solvent and stirred vigorously for 1 h. Then, after the THF solvent was completely dried, the resultant FTIR spectra for residual solids were acquired and compared with those for pristine HTMs.

Hole mobility of the HTL was measured by the space-charge-limited current (SCLC) method using hole-only devices with ITO/PEDOT:PSS/HTL/Au. Current−voltage measurements were performed in the voltage range of 0−2 V, and the results were fitted by the Mott-Gurney equation:

$$J_{\mathrm{SCLC}} = \frac{9}{8}\varepsilon\varepsilon_0\mu\frac{V^2}{L^3}$$

in which ε is the relative dielectric constant of the PTAA derivatives (2.7), ε_0 is the permittivity of free space (8.85×10^{14} F cm^{-1}), μ is the hole mobility, and V is the potential across the device ($V = V_{\mathrm{applied}} - V_{\mathrm{bi}} - V_{\mathrm{r}}$, where V_{bi} and V_{r} are the voltage drops induced by the built-in potential and the series resistance, respectively). L is the film thickness, evaluated by Park Systems NX-10 atomic force microscopy (AFM).

Device Fabrication

Indium tin oxide (ITO) substrates (15 Ω sq^{-1}, WOOYANG GMS) were sequentially cleaned for 20 min in the order of water+Mucasol solution (Schülke), water, acetone, and isopropanol (IPA) in the ultrasonic bath, respectively. For HTLs, PTAA and OEG-PTAA polymers were dissolved in chlorobenzene at 3 mg mL^{-1}. Then, those HTL solutions were deposited at 3000 rpm for 30s on the ITO substrate, followed by annealing on a hot plate at 100 °C for 5 min. For a perovskite layer, a perovskite precursor solution was prepared by dissolving 842 mg mL^{-1} of formamidinium lead iodide ($FAPbI_3$), 40.6 mg mL^{-1} of cesium lead bromide ($CsPbBr_3$), and 30 mg mL^{-1} of methylammonium chloride (MACl) in *N*,*N*-dimethyl formamide (DMF)/dimethyl sulfoxide (DMSO) (4:1 v/v) mixed solvent. The perovskite solution was deposited by two-step spin-coating process of 1000 rpm for 15 s and 5000 rpm for 35 s, respectively. During the second spin-coating step, 500 μL of ethyl acetate was quickly poured onto the substrate after 30 s. Then, the resultant intermediate phase film was successively annealed at 100 °C for 40 min and at 150 °C for 5 min on a hotplate. Next, the perovskite layers were treated by phenethylammonium iodide (PEAI) solution (1 mg mL^{-1} in IPA). Subsequently, C_{60} layer (18 nm) was thermally evaporated in vacuum on the PEAI-treated perovskite layer with an evaporation rate of 0.1-0.2 Å/s. After that, 0.2 wt% of polyethylenimine ethoxylated (PEIE) solution in IPA was spin-coated at 5000 rpm for 30 s on the top of C_{60} layer. Finally, an Ag electrode (100 nm) was deposited by thermal evaporation in vacuum.

For the best-performing device, a perovskite precursor solution was prepared by dissolving 889 mg mL^{-1} of $FAPbI_3$, 17.8 mg mL^{-1} of $CsPbBr_3$, and 33.3 mg mL^{-1} of MACl in DMF/DMSO (8:1 v/v) mixed solvents. The perovskite solution was deposited by two-step spin-coating process of 1000 rpm for 8 s and 5000 rpm for 15 s, respectively. During the second spin-coating step, 500 μL of ethyl acetate was quickly poured onto the substrate after 12 s. The intermediate phase film was put on a hotplate at 100 °C for 60 min. Next, the perovskite layers were treated

by PEAI solution (2 mg mL^{-1} in IPA). Subsequently, C_{60} layer was thermally evaporated in vacuum. Then, the tin oxide (SnO_2) layer was grown on the top of C_{60} layer at 80 °C in a commercial atomic layer deposition (ALD) system (CN-1, Atomic Premium). The precursors used were tetrakis(dimethylamino)tin (TDMASn) and deionized water for the tin and oxygen sources, respectively. Each ALD cycle included a sequential procedure of a dose of TDMASn for 0.5 s, followed by argon (Ar) purge for 10 s and a dose of H_2O for 0.1 s, followed by Ar purge for 10 s. Finally, an Ag electrode (100 nm) was deposited by thermal evaporation in vacuum.

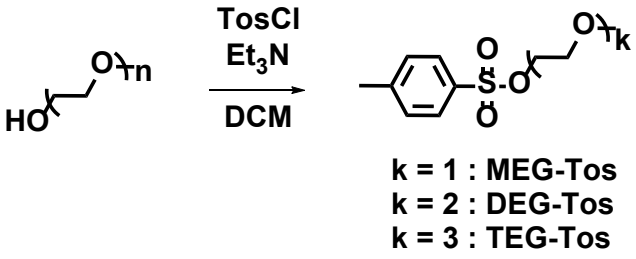

Scheme S1 The synthetic route for the OEG-Tos

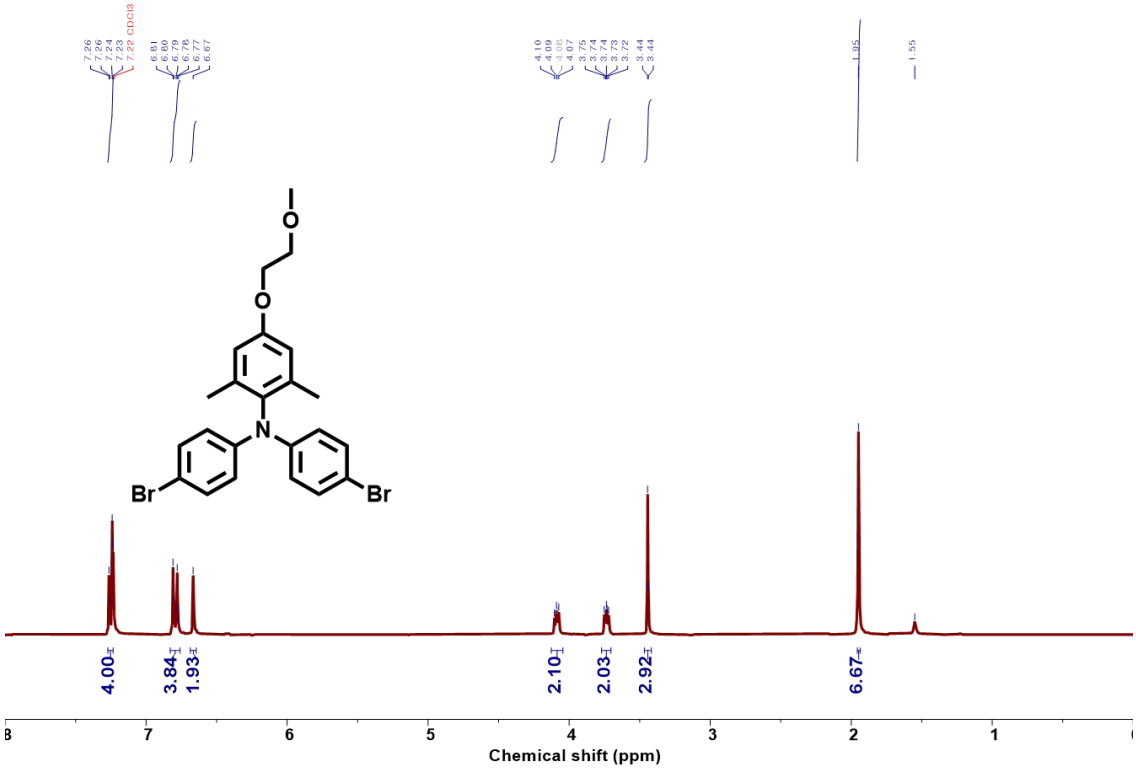

Fig. S1 ^{1}H NMR spectrum of the MEG-TAA

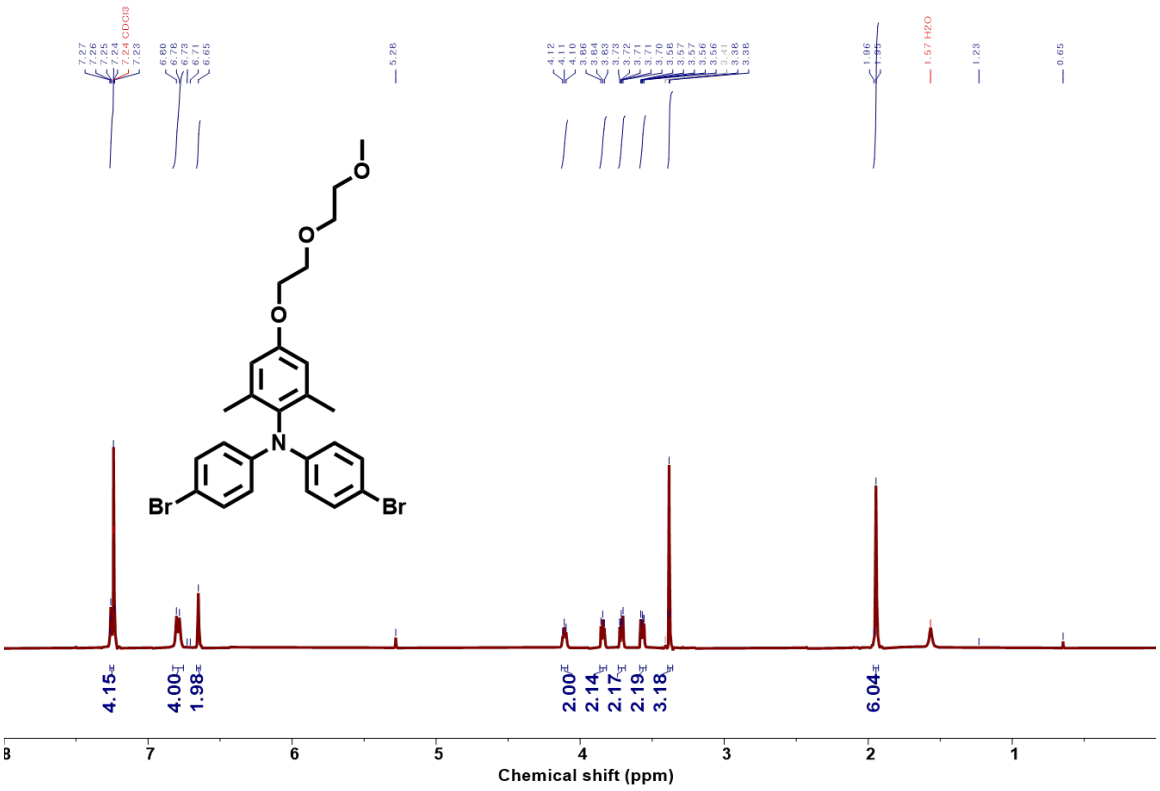

Fig. S2 ^{1}H NMR spectrum of the DEG-TAA

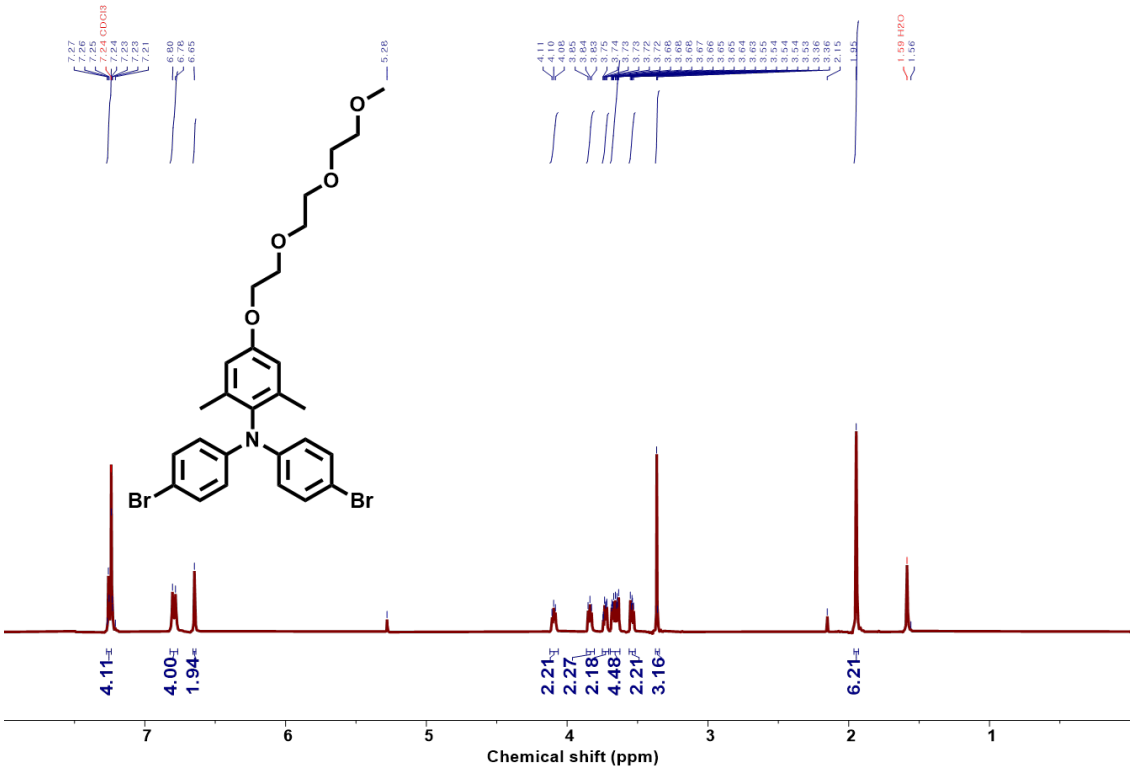

Fig. S3 ^{1}H NMR spectrum of the TEG-TAA

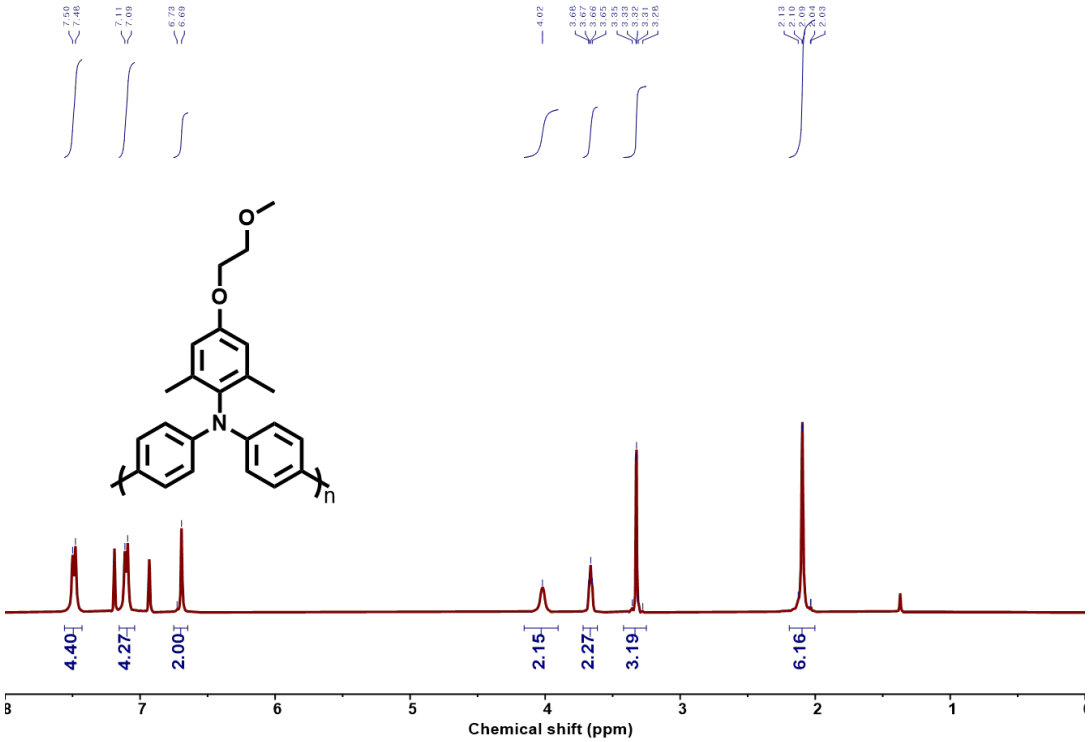

Fig. S4 ^{1}H NMR spectrum of the MEG-PTAA

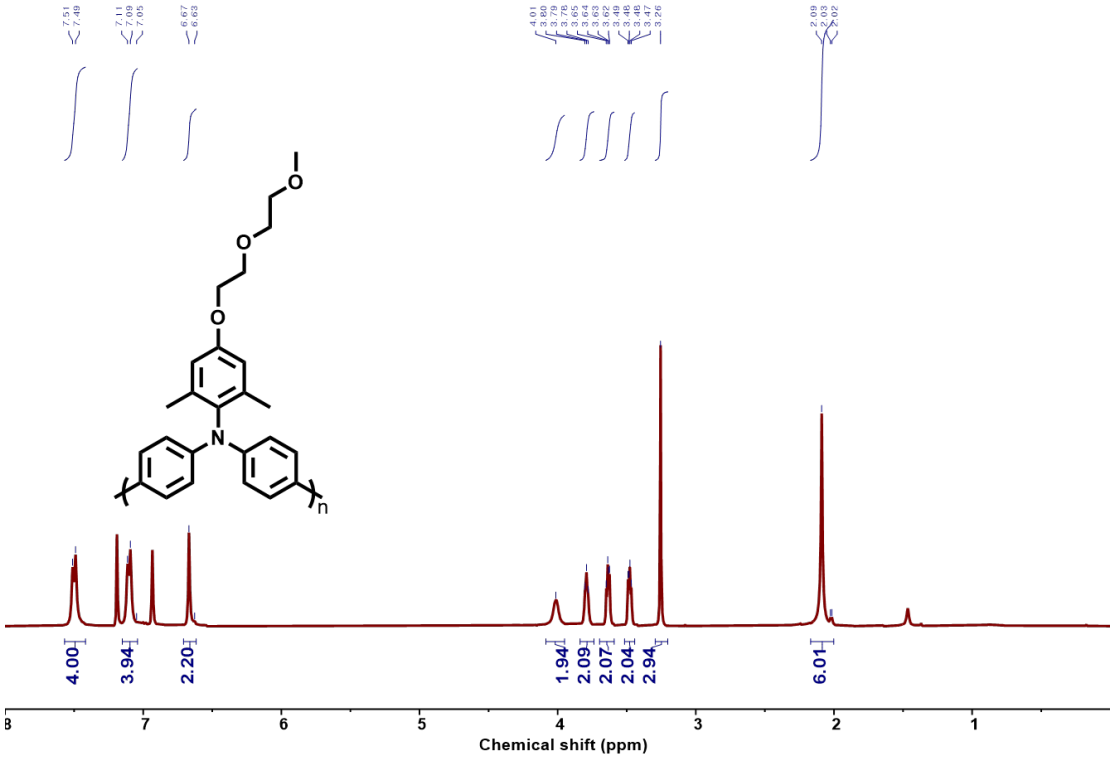

Fig. S5 ^{1}H NMR spectrum of the DEG-PTAA

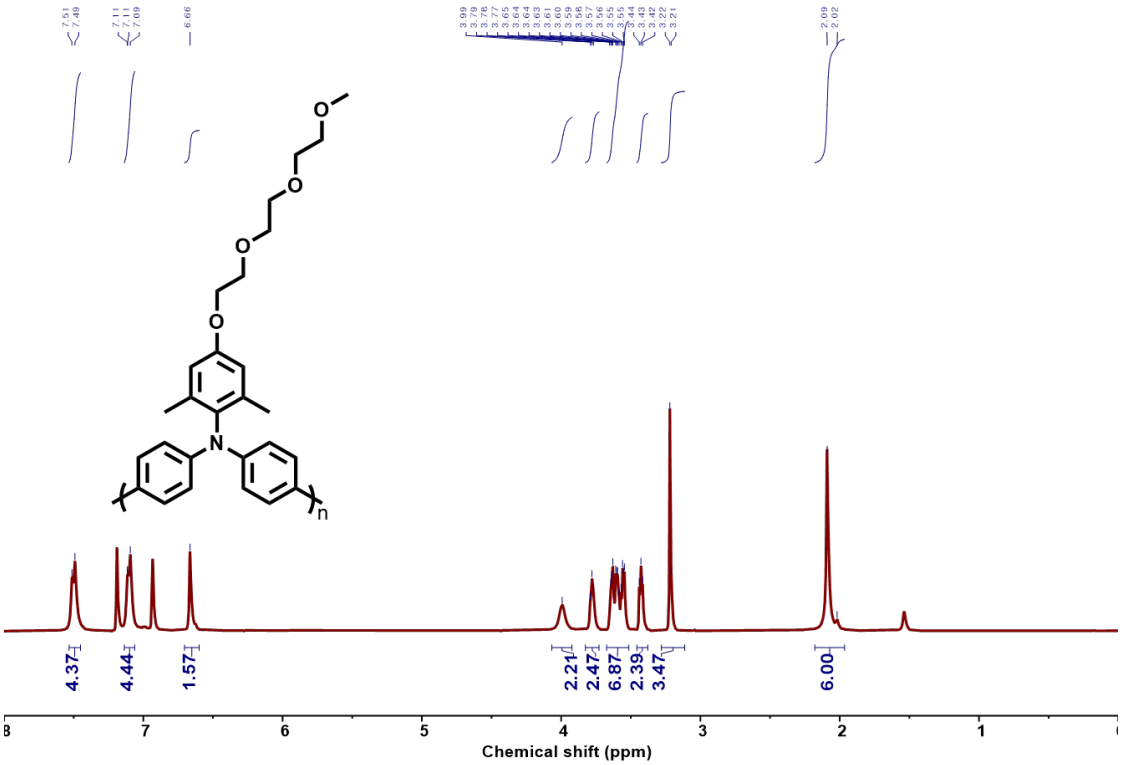

Fig. S6 ^{1}H NMR spectrum of the TEG-PTAA

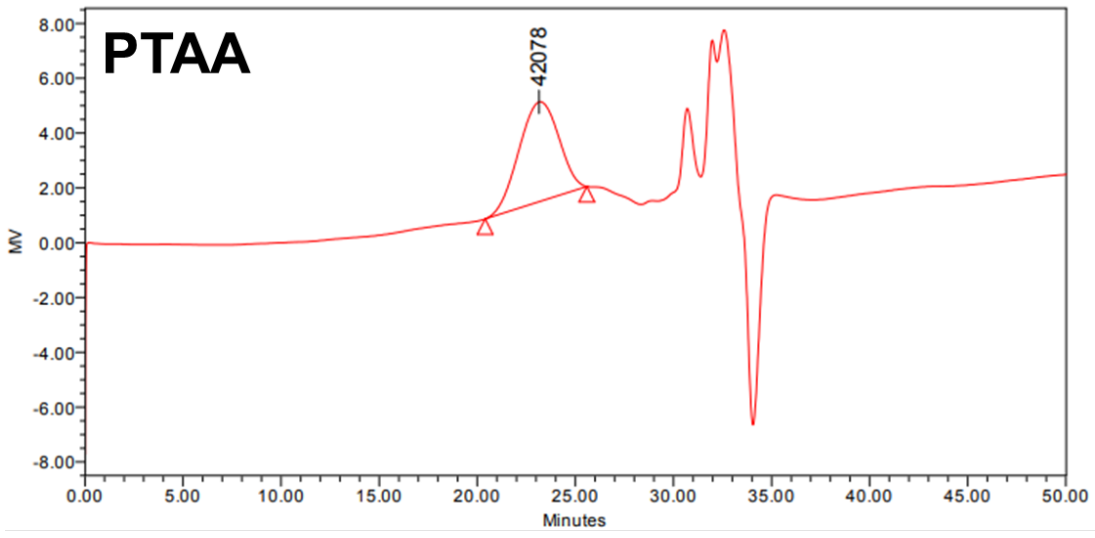

	Dist Name	Mn	Mw	MP	Mz	Mz+1	Mv	Polydispersity	MW Marker 1	MW Marker 2
1		36253	49368	42078	65726	83570		1.361743		

Fig. S7 SEC profile for the PTAA

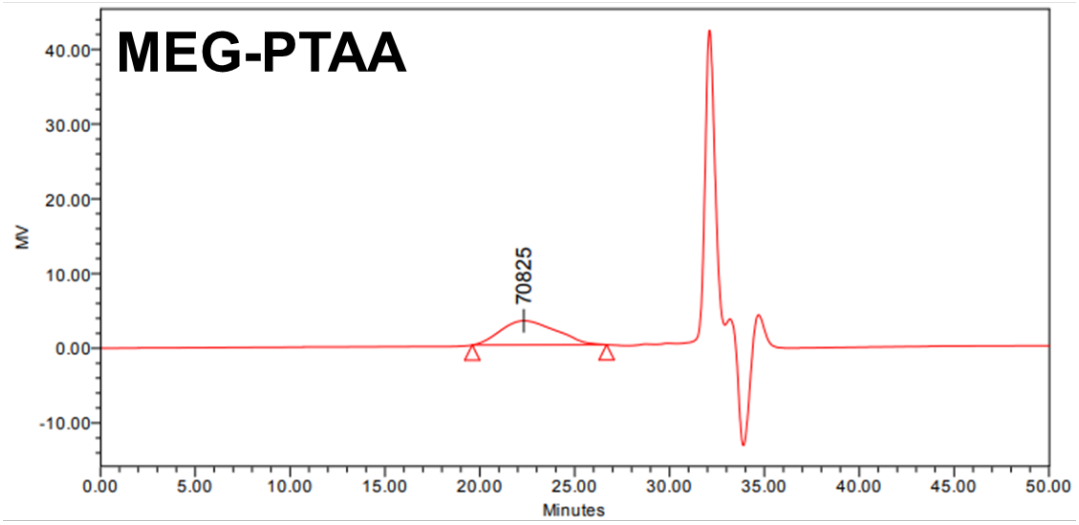

	Dist Name	Mn	Mw	MP	Mz	Mz+1	Mv	Polydispersity	MW Marker 1	MW Marker 2
1		39166	74160	70825	116618	156169		1.893498		

Fig. S8 SEC profile for the MEG-PTAA

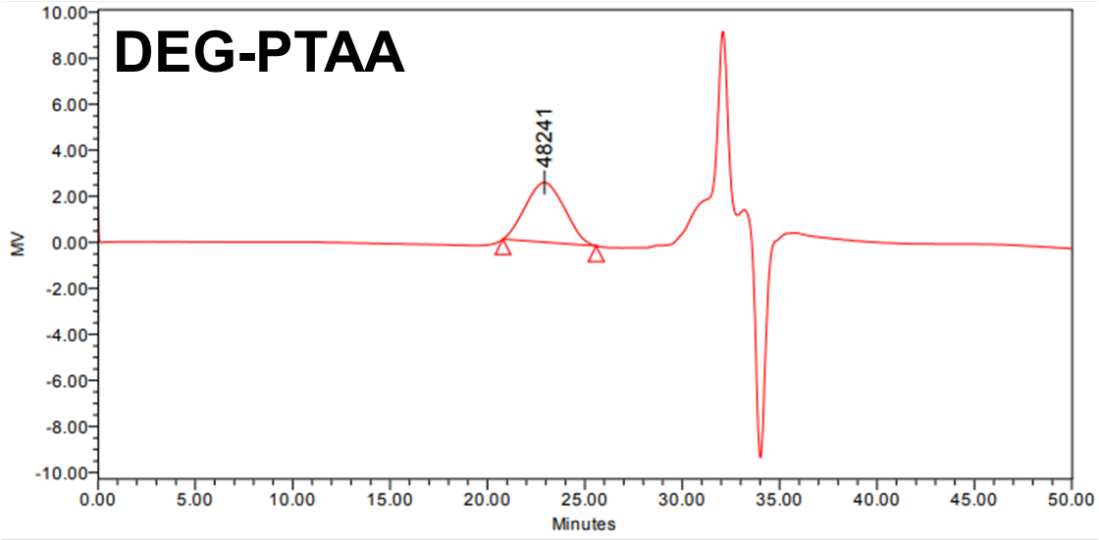

	Dist Name	Mn	Mw	MP	Mz	Mz+1	Mv	Polydispersity	MW Marker 1	MW Marker 2
1		39582	53340	48241	69080	84631		1.347580		

Fig. S9 SEC profile for the DEG-PTAA

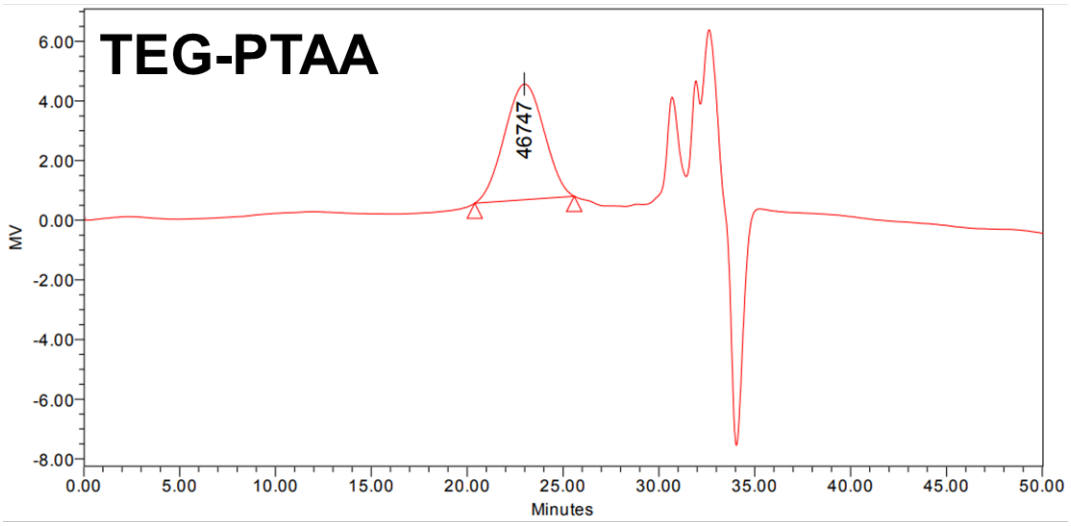

	Dist Name	Mn	Mw	MP	Mz	Mz+1	Mv	Polydispersity	MW Marker 1	MW Marker 2
1		39113	54348	46747	73179	93352		1.389525		

Fig. S10 SEC profile for the TEG-PTAA

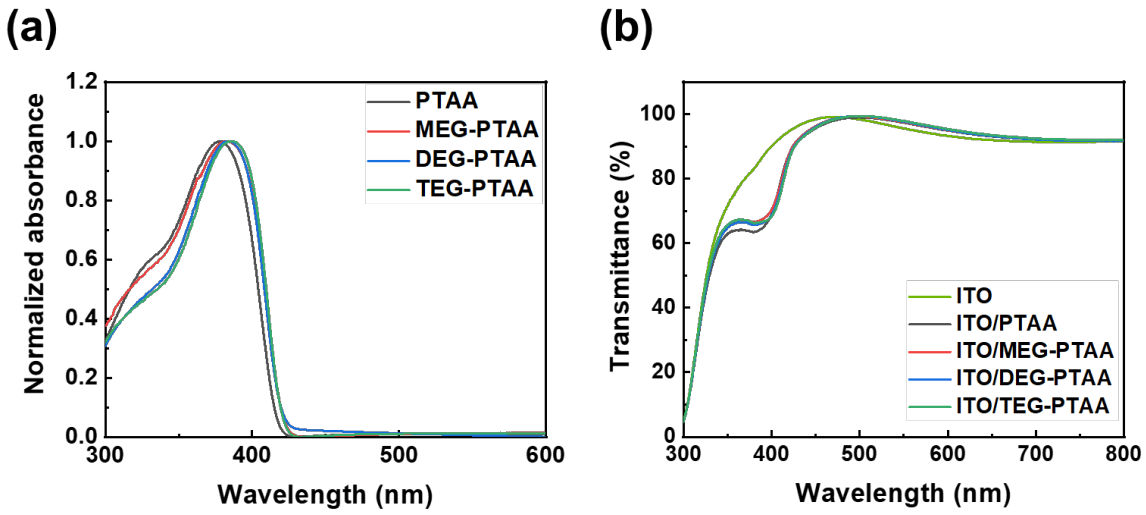

Fig. S11 (a) UV-Vis absorption spectra of the glass/HTL; (b) Optical transmittance spectra of the ITO and ITO/HTL

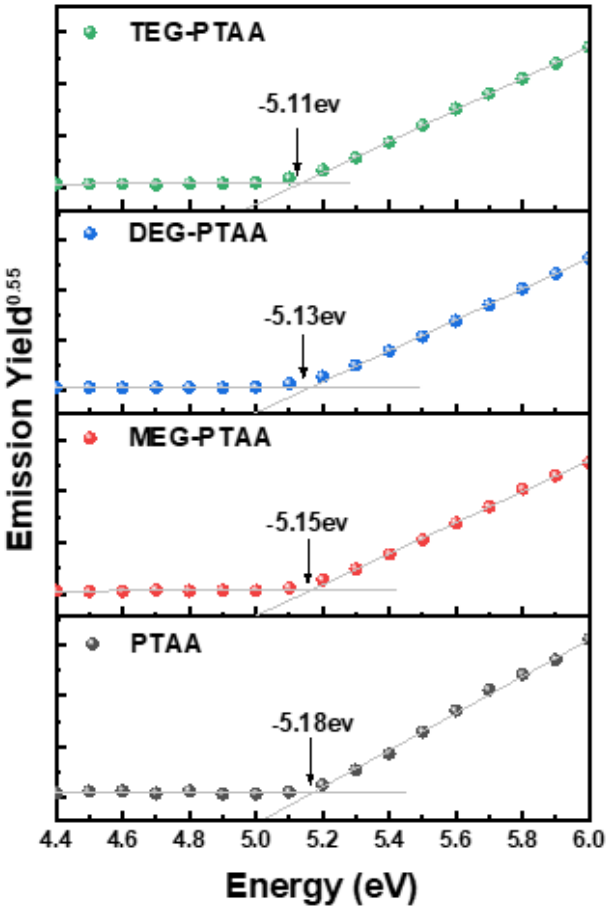

Fig. S12 PESA spectra of each HTL

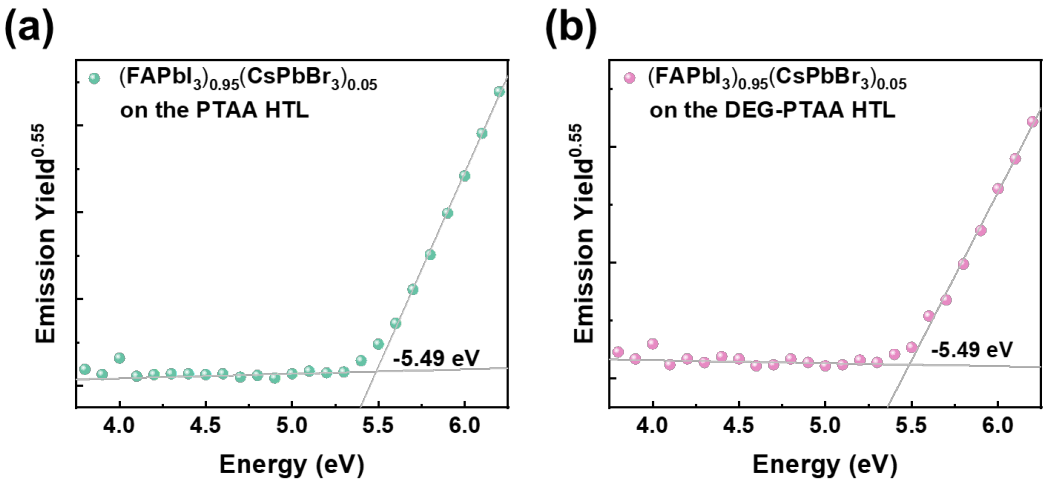

Fig. S13 PESA spectra of $(FAPbI_3)_{0.95}(CsPbBr_3)_{0.05}$ perovskite layer on the (a) PTAA and (b) DEG-PTAA HTLs

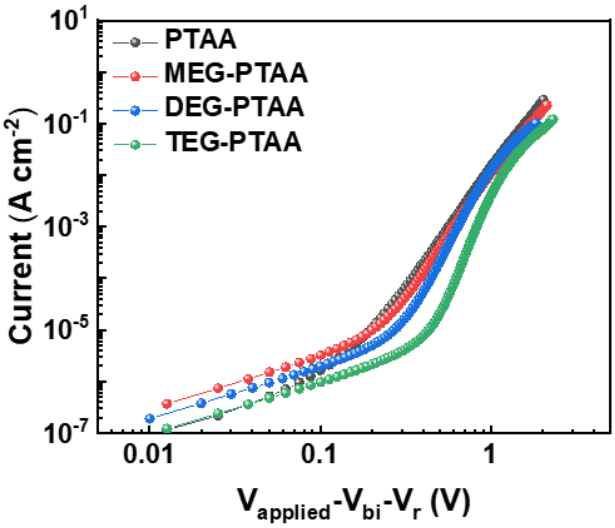

Fig. S14 SCLC curves of the PTAA and OEG-PTAA HTLs

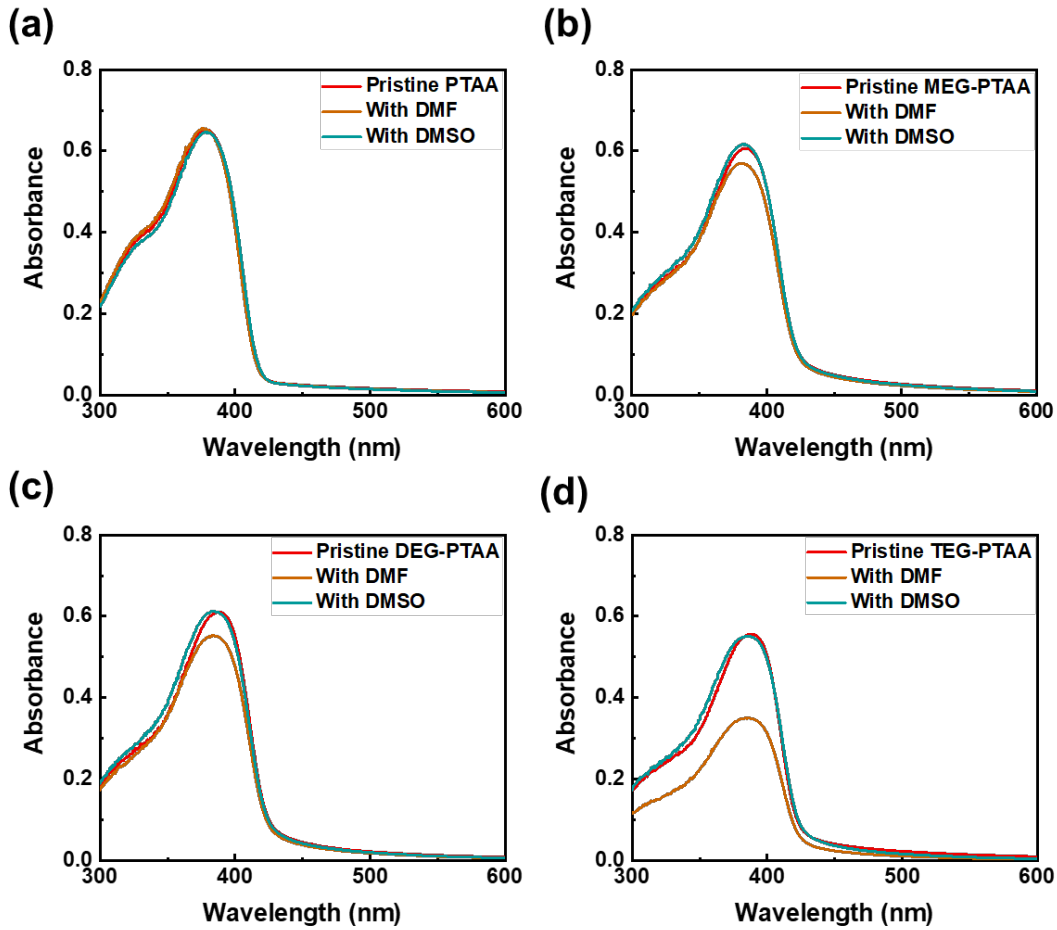

Fig. S15 UV-Vis absorption spectra of the (a) PTAA, (b) MEG-PTAA, (c) DEG-PTAA, and (d) TEG-PTAA in films before and after spin-coating process with pure DMF and DMSO

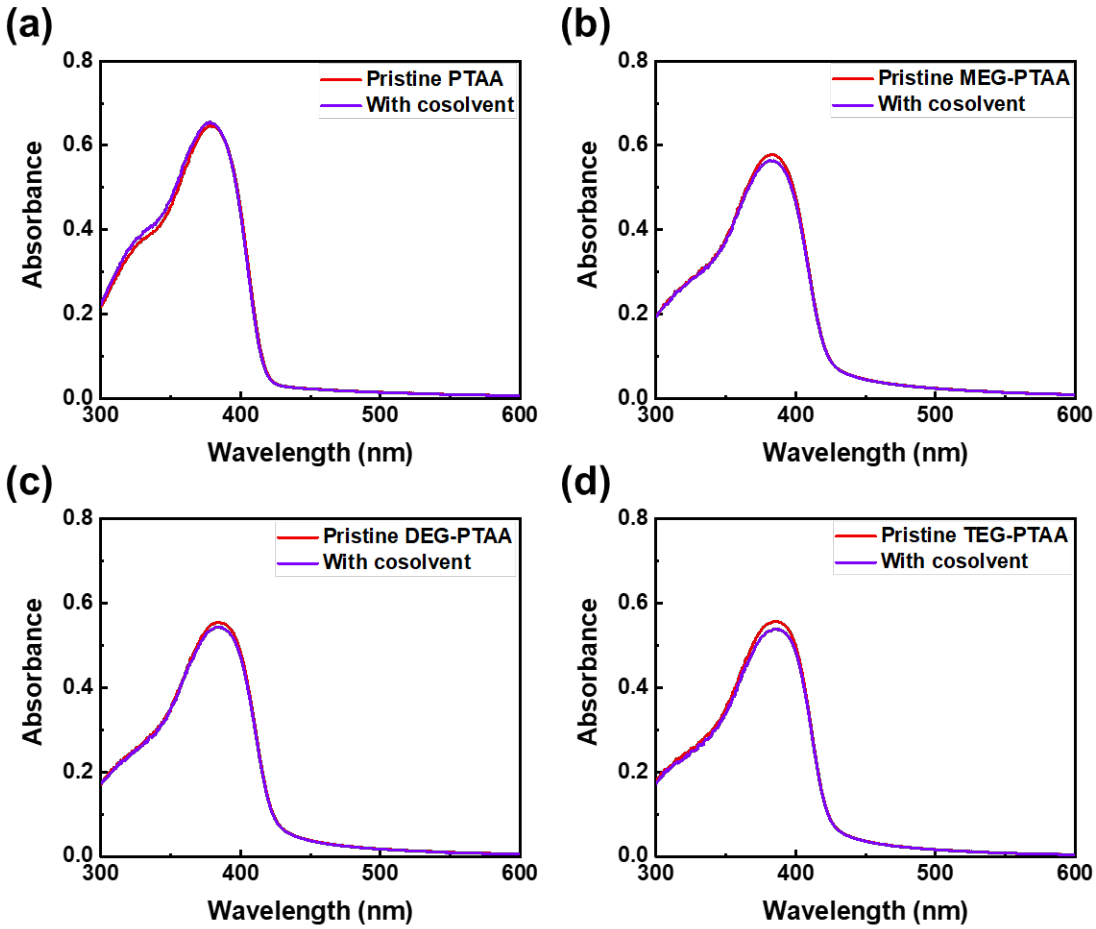

Fig. S16 UV-Vis absorption spectra of the (a) PTAA, (b) MEG-PTAA, (c) DEG-PTAA, and (d) TEG-PTAA in films before and after spin-coating process with the cosolvent (DMF and DMSO with a volume ratio of 4 to 1)

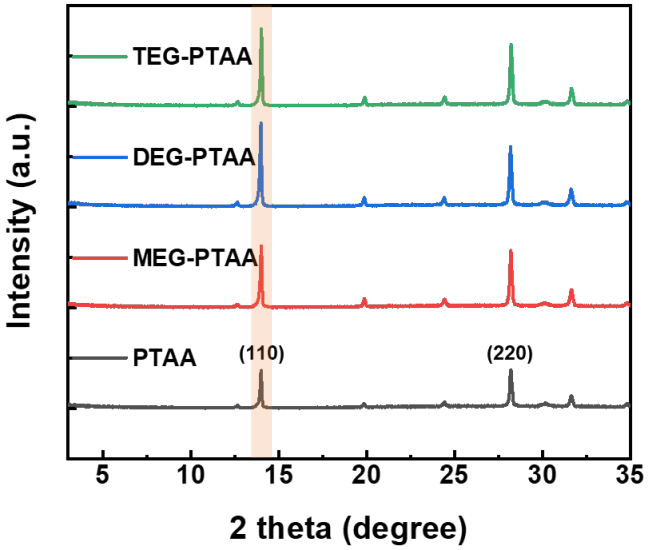

Fig. S17 XRD spectra of perovskite layers on each ITO/HTL

Table S1 Full width at half maximum **(**FWHM) value of (110) plane of the perovskite in the XRD spectra for each HTL

Substrate	**FWHM of (110)**
ITO/PTAA/Perovskite	0.120
ITO/MEG-PTAA/Perovskite	0.126
ITO/DEG-PTAA/Perovskite	0.127
ITO/TEG-PTAA/Perovskite	0.120

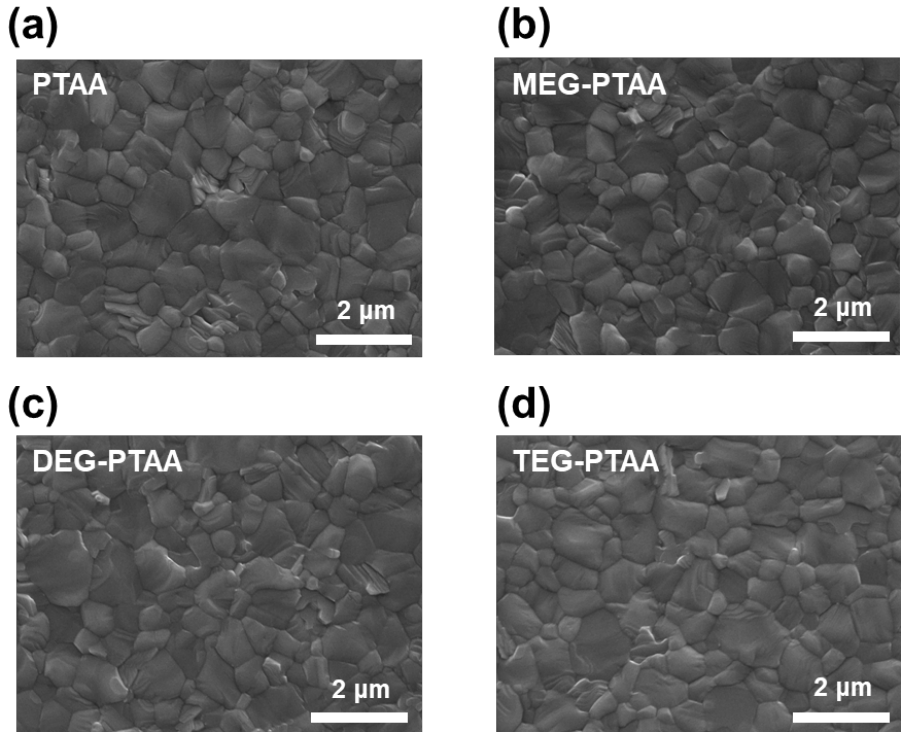

Fig. S18 SEM images of perovskite layers on the (a) ITO/PTAA, (b) ITO/MEG-PTAA, (c) ITO/DEG-PTAA, and (d) ITO/TEG-PTAA

Table S2 Binding energies of the Pb $4f_{5/2}$ and $4f_{7/2}$ peaks in XPS spectra for each HTL

Substrate	**Pb $4f_{5/2}$ [eV]**	**Pb $4f_{7/2}$ [eV]**
ITO/Perovskite	143.41	138.55
ITO/Perovskite/PTAA	143.43	138.57
ITO/Perovskite/MEG-PTAA	143.30	138.45
ITO/Perovskite/DEG-PTAA	143.25	138.40
ITO/Perovskite/TEG-PTAA	143.13	138.28

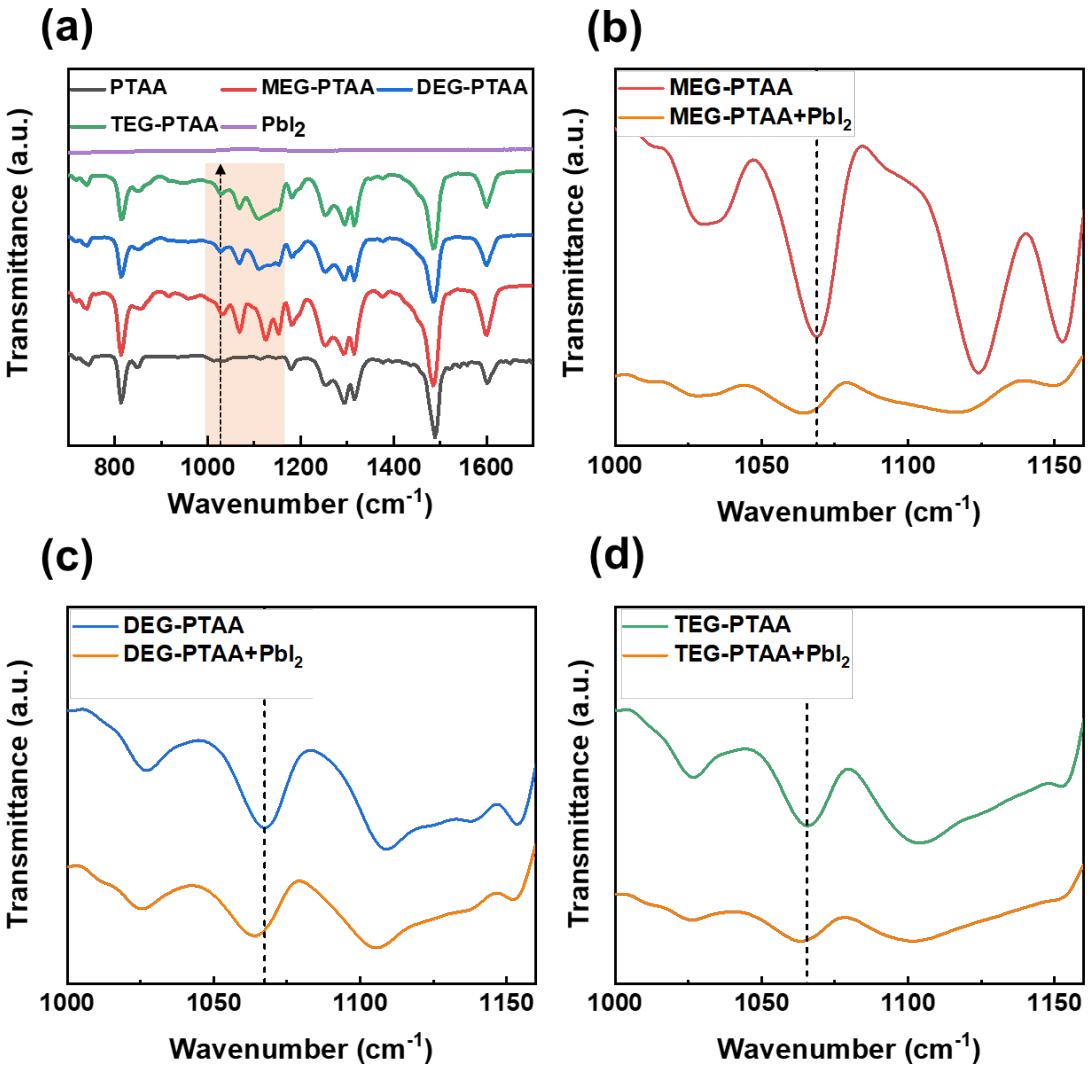

Fig. S19 (a) FTIR spectra of each pristine HTM and PbI_2; Stacked spectra of the pristine HTM and HTM:PbI_2 blend for the (b) MEG-PTAA, (c) DEG-PTAA, and (d) TEG-PTAA

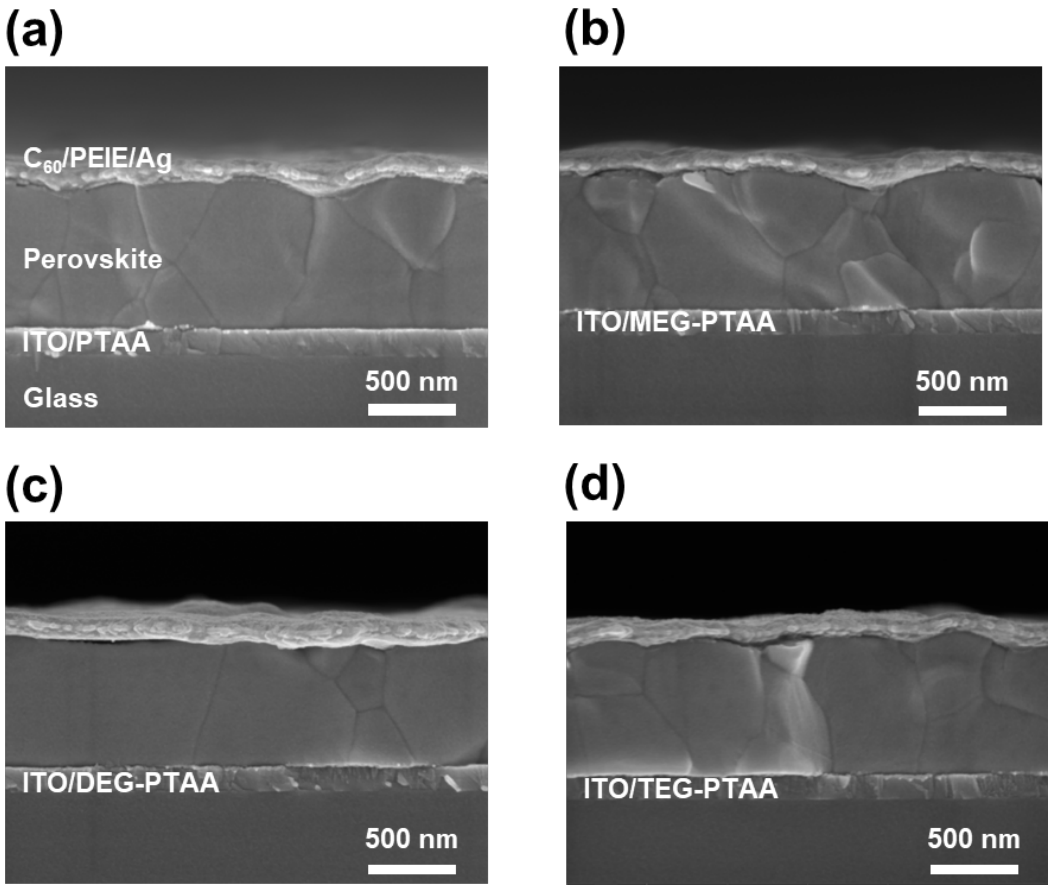

Fig. S20 Cross-sectional SEM images of the PSCs for the (a) PTAA, (b) MEG-PTAA, (c) DEG-PTAA and (d) TEG-PTAA

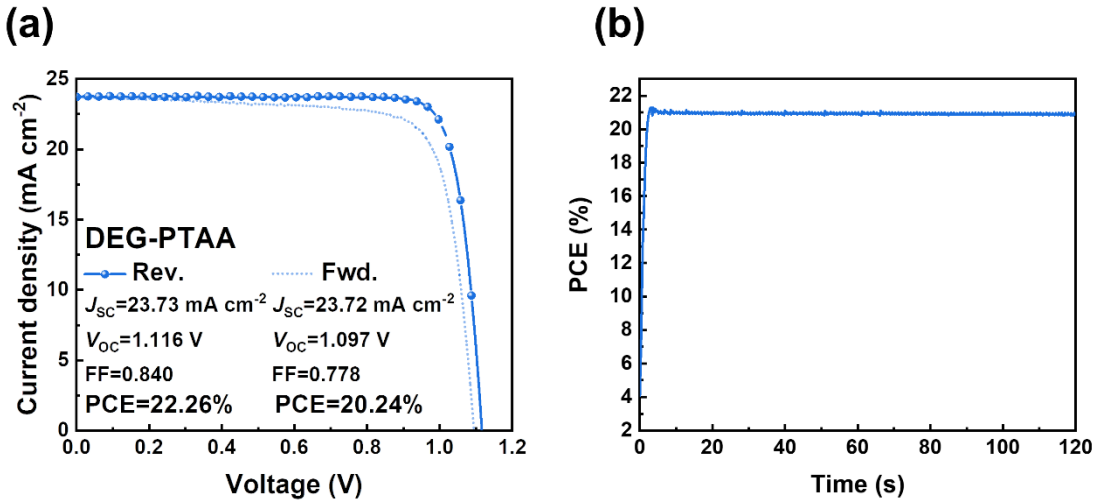

Fig. S21 (a) *J-V* curve and (b) MPP tracking spectrum of the PSC for the DEG-PTAA with additional device optimization and an anti-reflection film

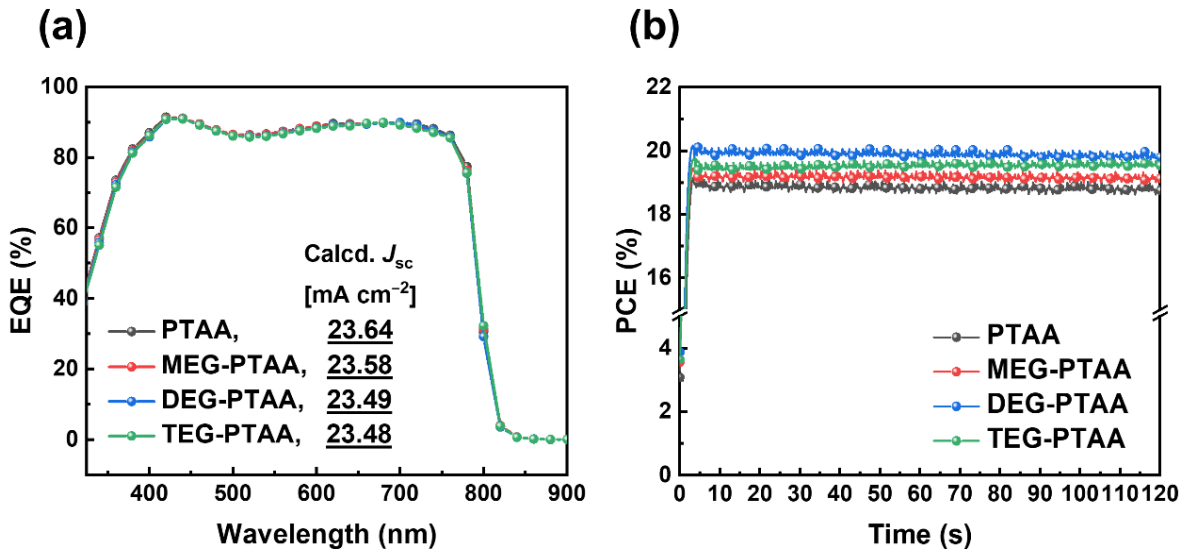

Fig. S22 (a) EQE spectra and (b) MPP tracking plots of the PSCs for each HTL

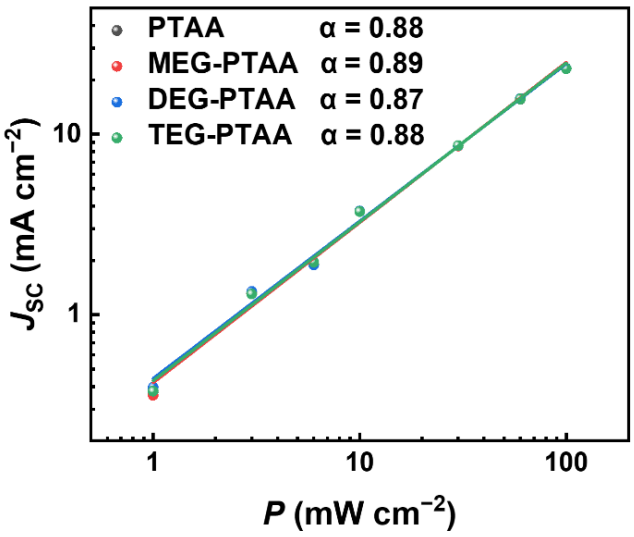

Fig. S23 Light intensity (P) versus J_{SC} plots of the PSCs for each HTL

Table S3 Results of bi-exponential components from TCSPC measurement for each HTL

Substrate	τ_1 [ns]	τ_2 [ns]
ITO/PTAA/Perovskite	56.3	237.8
ITO/MEG-PTAA/Perovskite	51.6	622.0
ITO/DEG-PTAA/Perovskite	73.3	1191.6
ITO/TEG-PTAA/Perovskite	117.1	1022.1

References

1. Y. Kim, G. Kim, N. J. Jeon, C. Lim, J. Seo and B. J. Kim, *ACS Energy Lett.*, 2020, **5**, 3304-3313.